molecules

MDPI

Article

Rate Coefficients of the Reactions of Fluorine Atoms with H_2S and SH over the Temperature Range 220–960 K

Yuri Bedjanian

Institut de Combustion, Aérothermique, Réactivité et Environnement (ICARE), CNRS, CEDEX 2, 45071 Orléans, France; yuri.bedjanian@cnrs-orleans.fr; Tel.: +33-238255474

Abstract: Reaction F + H_2S→SH + HF (1) is an effective source of SH radicals and an important intermediate in atmospheric and combustion chemistry. We employed a discharge-flow, modulated molecular beam mass spectrometry technique to determine the rate coefficient of this reaction and that of the secondary one, F + SH→S + HF (2), at a total pressure of 2 Torr and in a wide temperature range 220–960 K. The rate coefficient of Reaction (1) was determined directly by monitoring consumption of F atoms under pseudo-first-order conditions in an excess of H_2S. The rate coefficient of Reaction (2) was determined via monitoring the maximum concentration of the product of Reaction (1), SH radical, as a function of [H_2S]. Both rate coefficients were found to be virtually independent of temperature in the entire temperature range of the study: $k_1 = (1.86 \pm 0.28) \times 10^{-10}$ and $k_2 = (2.0 \pm 0.40) \times 10^{-10}$ cm^3 molecule^{-1} s^{-1}. The kinetic data from the present study are compared with previous room temperature measurements.

Keywords: fluorine atom; hydrogen sulfide; H_2S; SH; kinetics; rate coefficient

Citation: Bedjanian, Y. Rate Coefficients of the Reactions of Fluorine Atoms with H_2S and SH over the Temperature Range 220–960 K. *Molecules* **2022**, *27*, 8365. https://doi.org/10.3390/molecules27238365

Academic Editors: Marzio Rosi and Stefano Falcinelli

Received: 24 October 2022
Accepted: 24 November 2022
Published: 30 November 2022

1. Introduction

Reactions of atomic fluorine, as a rule, are extremely fast, with rate coefficients often approaching the bimolecular collision frequency [1]. The rapidity of the elementary reactions of the F atoms arouses, in addition to theoretical interest, a practical interest for these reactions, in particular for the generation of active species (atoms and radicals) in laboratory gas-phase kinetic studies. For example, reactions of atomic fluorine with H_2O [2], H_2O_2 [3], CH_4 [4], and HNO_3 [5] are often used as a source of OH, HO_2, CH_3, and NO_3 radicals, respectively. In the present work we report the results of an experimental study of the reactions of F atoms with hydrogen sulfide:

$$F + H_2S \rightarrow SH + HF \quad (1)$$

Reaction (1) is a convenient and effective source of SH radicals, an important intermediate in combustion [6] and atmospheric chemistry [7]. The experimental study of the fast elementary reactions of F atoms is challenging, in particular, due to the presence of a rapid secondary chemistry. The secondary reaction, occurring in the F + H_2S chemical system,

$$F + SH \rightarrow S + HF \quad (2)$$

was also investigated as a part of this study.

The kinetic information available for Reactions (1) and (2) is extremely scarce. There are no data on the temperature dependence of the reaction rate coefficients. One theoretical study [8] and only three relative [9–11] and one absolute measurement [12] of the rate coefficient of Reaction (1) are available, all realized at room temperature. The reported room temperature values of the rate coefficient differ by a factor of nearly 1.5. For Reaction (2), there is only one previous measurement, also at room temperature [12].

The objective of the present work was to determine the rate coefficients of the title reactions over a wide temperature range, T = 220–960 K, in order to provide a new kinetic data set for use in laboratory studies and, potentially, in theoretical reaction rate calculations.

2. Experimental

Experiments have been carried out at total pressure of 2 Torr of Helium in a flow tube reactor, employed in the laminar flow regime (Reynolds number < 10), and combined with a modulated molecular beam quadrupole mass spectrometer for the detection of the gas phase species. The experimental setup has been used extensively in the past, in particular, to study the kinetics and products of the reaction involving atomic fluorine [4,5,13–16]. Briefly, it consists of the gas introduction vacuum lines, the flow tube reactor, and the differentially pumped stainless steel high-vacuum chamber which houses the quadrupole mass spectrometer (Balzers, QMG 420, Balzers Aktiengesellschaft, Liechtenstein). Gas phase molecules sampled from the flow reactor are modulated by a tuning-fork chopper (35 Hz), ionized through impact with high kinetic energy electrons (18–30 eV, in this study) emitted by the ion source of the mass spectrometer and detected using an electron multiplier. Subsequently, the mass spectrometric signals are filtered and amplified with a lock-in amplifier and recorded for further analysis.

Two different flow reactors were used depending on temperature of the kinetic measurements. A low-temperature flow reactor covered the temperature range 220–320 K and consisted of a Pyrex tube (45 cm in length, 2.4 cm i.d.) with an outer jacket through which a temperature-regulated fluid was circulated. To minimize wall-loss of active species (F atoms and SH radicals), the inner surface of the reactor as well as the mobile injector were coated with halocarbon wax. A high-temperature flow reactor (Figure 1), used over the temperature range 300–960 K, consisted of a quartz tube (45 cm in length, 2.5 cm i.d.), where the temperature was controlled with electrical heating elements [17]. The temperature in the reactor was measured with a K-type thermocouple positioned in the middle of the reactor in contact with its outer surface. A temperature gradient along the flow tube measured with a thermocouple inserted in the reactor through the movable injector was found to be less than 1%.

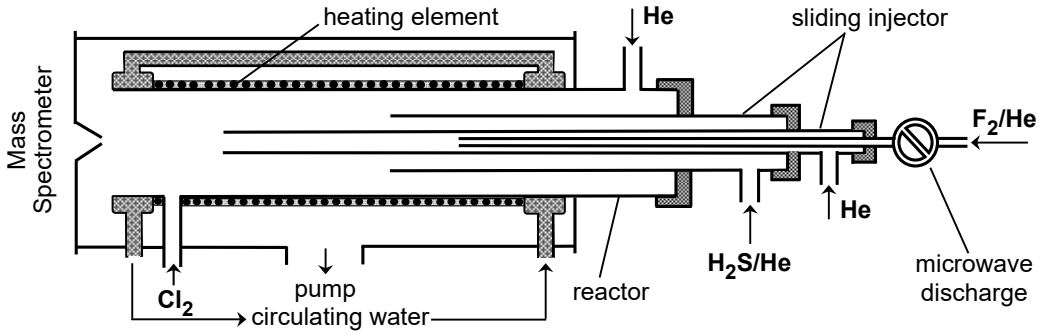

Figure 1. High-temperature flow reactor: configuration used in the measurements of the rate coefficient of reaction (1).

Fluorine atoms were produced by discharging trace amounts of F_2 in He in a microwave cavity (microwave generator Microtron 2000, 75 W, 2450 MHz, Electro-Medical Supplies Ltd., Wantage Oxfordshire England). To reduce F atom reactions with a glass surface inside the microwave cavity, a ceramic (Al_2O_3) tube was inserted in this part of the injector. It was verified by mass spectrometry that more than 95% of F_2 was dissociated in the microwave discharge. The fluorine atoms were detected either as FCl (FCl^+, m/z = 54) or as FBr at m/z = 98/100 (FBr^+), after being scavenged in rapid reactions with excess Cl_2 or Br_2, respectively, added at the end of the reactor 5 cm upstream of the sampling cone:

$$F + Cl_2 \rightarrow Cl + FCl \quad (3)$$

$k_3 = 6.0 \times 10^{-11}$ cm^3 molecule^{-1} s^{-1} (T = 180–360 K) [18].

$$F + Br_2 \rightarrow Br + FBr \quad (4)$$

$k_4 = 1.28 \times 10^{-10}$ cm^3 molecule^{-1} s^{-1} (T = 299–940 K) [14].

Absolute concentrations of F atoms were determined through their titration in Reactions (3) and (4) from the consumed fraction of Cl_2 and Br_2 ([F] = Δ[Cl_2] = [FCl] and [F] = Δ[Br_2] = [FBr]), respectively.

A similar approach was used to monitor two other labile species, S atoms and SH radicals, detected as BrS (BrS^+, m/z = 111/113) and BrSH at m/z = 112/114 ($BrSH^+$), respectively:

$$S + Br_2 \rightarrow Br + BrS \quad (5)$$

$k_5 = 9.5 \times 10^{-11}$ cm^3 molecule^{-1} s^{-1} (T = 298 K) [19].

$$SH + Br_2 \rightarrow Br + BrSH \quad (6)$$

$k_6 = 5.7 \times 10^{-11} \exp(160/T)$ cm^3 molecule^{-1} s^{-1} (T = 273–373 K) [20].

Absolute calibration of the mass spectrometric signals of BrSH was carried out as follows. First, the F atoms were titrated with an excess of Br_2 in the main reactor, which led to the formation of FBr ($[FBr]_0$). Then, the same concentration of F atoms was titrated with a mixture of Br_2 and H_2S resulting in the formation of FBr ([FBr]) and SH in Reactions (4) and (1), respectively. In the presence of Br_2, SH radicals are rapidly converted to BrSH ([BrSH]) according to Reaction (6). The absolute concentration of BrSH was determined as [BrSH] = $[FBr]_0$ − [FBr]. This calibration procedure avoids possible complications due to the rapid self-reaction of SH radicals:

$$SH + SH \rightarrow S + H_2S \quad (7)$$

$k_7 = 1.2 \times 10^{-11}$ cm^3 molecule^{-1} s^{-1} (T = 298 K) [21,22].

In several experiments, SH was detected directly at its parent peak (SH^+, m/z = 33). In this case, the SH signals should be corrected for the contribution of H_2S at m/z = 33 due to the dissociative ionization of H_2S in the ion source of the mass spectrometer. At an electron energy of 18 eV, the contribution of H_2S at m/z = 33 was $\leq$4% of the intensity of its parent peak (H_2S^+, m/z = 34).

The purities of the gases used were as follows: Br_2 > 99.99% (Aldrich); Cl_2 (>99%; Ucar); F_2, 5% in helium (Alphagaz); and H_2S > 99.5% (Alphagaz). Absolute concentrations of all stable species (H_2S, F_2, Cl_2, and Br_2) were derived from the measured flow rates of their manometrically prepared gas mixtures. He (the carrier gas) was taken directly from a high-pressure tank and had stated purity better than 99.999% (Alphagaz).

3. Results and Discussion

3.1. Rate Coefficient of Reaction (1)

The rate coefficient of Reaction (1), k_1, was measured in an absolute way under pseudo-first order conditions in an excess H_2S over F atoms ($[F]_0 = (0.6–1.2) \times 10^{11}$ molecule cm^{-3}, $[H_2S]/[F]_0$ = 2–35). The consumption of the excess reactant, H_2S, in Reaction (1) generally did not exceed a few percent, although reaching up to 20% in a few kinetic runs. In all cases, the average concentration of H_2S along the reaction zone was used in the calculations. In this series of experiments, Cl_2 ($[Cl_2] \approx 4 \times 10^{13}$ molecule cm^{-3}) was added at the end of the reactor (Figure 1) and F atoms were detected as FCl. In fact, measurements of the very high rate coefficient of Reaction (1) required the use of low concentrations of F atoms and the sensitivity of the mass spectrometer towards FCl was much better than that of FBr. The concentration vs. time profiles of both F-atom and H_2S were monitored by changing the position of the movable injector (Figure 1). The distance between the injector head and the Cl_2 introduction point (5 cm upstream of the sampling cone) was converted into reaction time using the linear flow velocity (2190–2830 cm s^{-1}) of the gas mixture

in the reactor. Figure 2 shows typical data obtained in this manner. The linearity of the semilogarithmic plots in Figure 2 clearly illustrates that the F-atom decays are first order, $[F] = [F]_0 \times \exp(-k_1' \times t)$, where $k_1' = k_1 \times [H_2S]$.

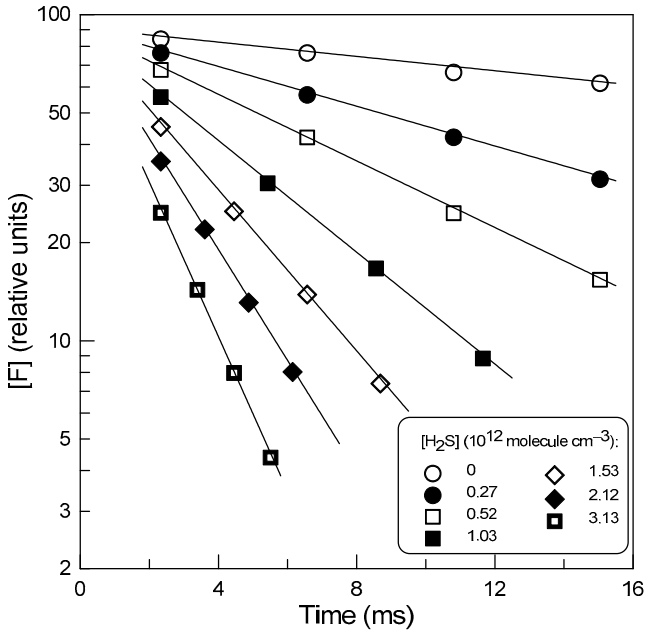

Figure 2. Typical F-atom decay profiles observed in the presence of different concentrations of H_2S at T = 295 K.

Examples of the second-order plots observed at different temperatures are shown in Figure 3.

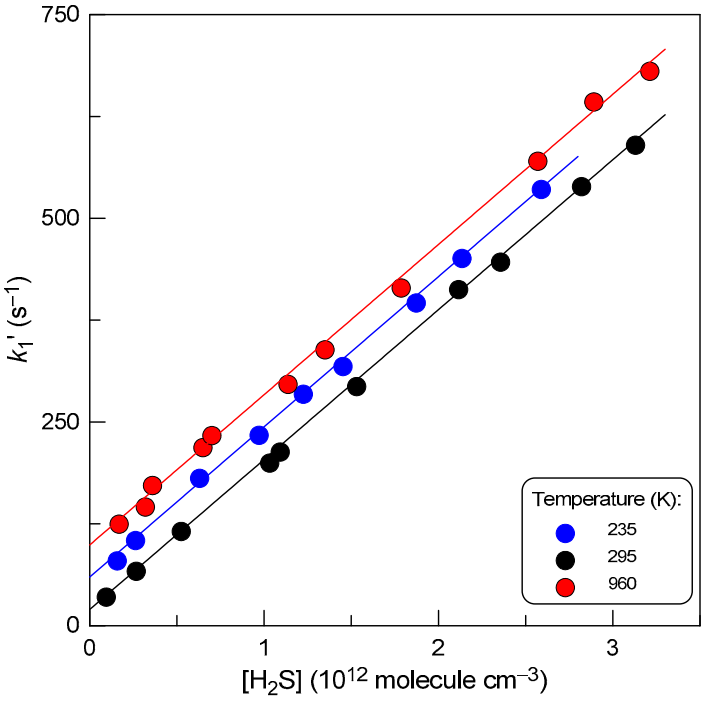

Figure 3. Dependence of the pseudo-first order rate constant, $k_1' = k_1[H_2S]$, on the concentration of H_2S at different temperatures. For clarity, k_1' data at T = 235 and 960 K are Y-shifted by 35 and 50 s^{-1}, respectively.

A linear least-squares fit of these data at each temperature gave the bimolecular rate coefficient. A summary of the absolute measurements of k_1 is given in Table 1. The combined uncertainty on k_1 was estimated to be around 15% by adding in quadrature statistical error ($\leq$2%) and those on the measurements of the absolute concentration of H_2S (~10%), flows (3%), pressure (2%), and temperature (1%). It is important to note that the current measurements of k_1 were not affected by the fast secondary Reaction (2), given that the values of k_1 and k_2 are close (see below) and that [SH] $\leq \Delta$[F] << [H_2S] under experimental conditions of the measurements.

Table 1. Experimental conditions and results of the measurements of the rate coefficient of reaction (1).

T (K) [a]	[H_2S] [b]	k_1 [c]	Reactor Surface [d]
220	0.11–2.87	1.94	HW
235	0.16–2.59	1.84	HW
250	0.19–2.26	1.86	HW
270	0.15–2.51	1.89	HW
295	0.27–3.13	1.84	HW
305	0.17–2.60	1.84	Q
320	0.13–2.95	1.85	HW
360	0.26–3.04	1.89	Q
410	0.16–2.03	1.89	Q
475	0.16–2.60	1.89	Q
575	0.14–4.44	1.83	Q
720	0.15–2.82	1.83	Q
960	0.17–3.21	1.84	Q

[a] 7–11 kinetic runs with different [H_2S] at each temperature, $[F]_0$ = (0.6–1.2) $\times$ 10^{11} cm^{-3}. [b] Units of 10^{12} molecule cm^{-3}; [c] units of 10^{-10} cm^3 molecule^{-1} s^{-1}; statistical 2σ uncertainty is $\leq$2%; total estimated uncertainty is 15%; [d] HW: halocarbon wax; Q: quartz.

The present data for k_1 are plotted as a function of temperature in Figure 4 together with previous room temperature measurements [9–12]. In the single direct measurement of k_1, Schölne et al. [12] used an experimental setup similar to that of the present study and determined the rate coefficient of Reaction (1) from the kinetics of H_2S consumption in an excess of F atoms, k_1 ($\pm1\sigma$) = (1.28 $\pm$ 0.04) $\times$ 10^{-10} cm^3 molecule^{-1} s^{-1}. This value is lower by a factor of 1.45 than the current measurement. Schölne et al. [12] also performed several experiments with an excess of H_2S relative to F atoms. The rate coefficient of Reaction (1), determined under these conditions from the kinetics of HF formation, was k_1 ($\pm1\sigma$) = (1.7 $\pm$ 0.4) $\times$ 10^{-10} cm^3 molecule^{-1} s^{-1}, which agrees very well with the present measurements. Smith et al. [10], measuring the relative HF infrared emission intensities from the reactions of F atoms with different compounds, determined k_1 relative to the rate coefficient of Reaction (8), k_1/k_8 = 2.0 $\pm$ 0.2:

$$F + CH_4 \rightarrow CH_3 + HF \quad (8)$$

k_8 = 1.28 $\times$ 10^{-10} exp(−219/T) cm^3 molecule^{-1} s^{-1} (T = 220–960 K) [4].

A much higher value for this ratio, k_1/k_8 = 3.2 $\pm$ 0.3, can be extracted from the work of Williams and Rowland [9], who studied a number of competitive reactions involving thermalized ^{18}F atoms. Persky [11], monitoring the decays of H_2S and CH_4 in reactions with F atoms in a flow reactor, determined k_1/k_8 = 2.35 $\pm$ 0.05 ($\pm2\sigma$). The relative rate data placed on an absolute basis with recently updated k_8 = 6.14 $\times$ 10^{-11} cm^3 molecule^{-1} s^{-1} (T = 298 K) [4] provide the following values for k_1: (1.23 $\pm$ 0.25) $\times$ 10^{-10} [10], (1.44 $\pm$ 0.30) $\times$ 10^{-10} [11], and (1.96 $\pm$ 0.40) $\times$ 10^{-10} cm^3 molecule^{-1} s^{-1} [9] with 20% uncertainty including 15% uncertainty on the rate coefficient of the reference Reaction (8) [4]. The last two values of k_1 agree with the present measurements within the experimental uncertainties.

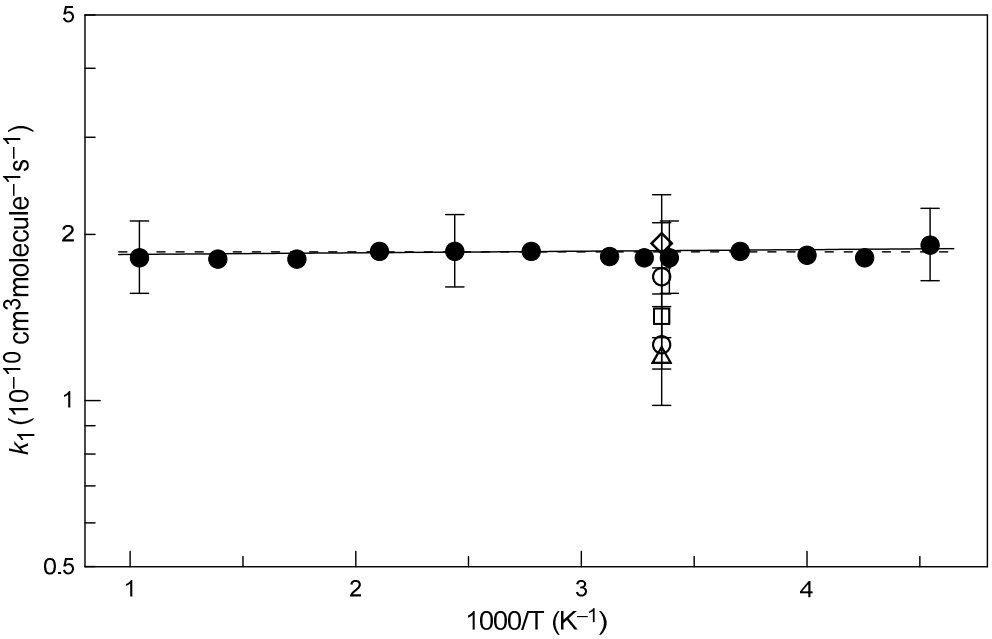

Figure 4. Summary of the measurements of k_1: diamonds, Williams and Rowland [9]; triangles, Smith et al. [10]; open circles, Schölne et al. [12]; squares, Persky [11]; filled circles, this work. Uncertainties shown for selected present measurements of k_1 correspond to 15%.

The continuous line in Figure 4 represents an exponential fit to the present data: $k_1 = (1.83 \pm 0.03) \times 10^{-10} \exp((7 \pm 4)/T)$ cm^3 molecule^{-1} s^{-1} with statistical 2σ uncertainties on the precision of the fit. The experimental data for k_1 are also well described (dashed line in Figure 4) with a temperature-independent value of $k_1 = (1.86 \pm 0.28) \times 10^{-10}$ cm^3 molecule^{-1} s^{-1}. We estimate the rate coefficient to be accurate within 15% over the investigated temperature range 220–960 K.

3.2. Rate Coefficient of Reaction (2)

The rate coefficient of F-atom reaction with SH was determined relative to that of Reaction (1). Kinetics of H_2S and SH were monitored in an excess of F atoms over H_2S. An example of the observed kinetic runs is shown in Figure 5. The simulated concentration vs. time profiles shown in Figure 5 were obtained within a simple mechanism including Reactions (1), (2) and (7) and wall loss of the active species involved, F + H_2S→SH + HF, $k_1 = 1.86 \times 10^{-10}$ cm^3 molecule^{-1} s^{-1} (this work); F + SH→S + HF, $k_2 = 1.90 \times 10^{-10}$ cm^3 molecule^{-1} s^{-1} (fit), SH + SH→S + H_2S, $k_7 = 1.2 \times 10^{-11}$ cm^3 molecule^{-1} s^{-1} [21,22]:

$$\text{F + wall loss } k_9 = 20 \text{ s}^{-1} \text{ (this work)} \quad (9)$$

$$\text{SH + wall}\rightarrow\text{loss } k_{10} = 35 \text{ s}^{-1} \text{ (this work)} \quad (10)$$

$$\text{S + wall}\rightarrow\text{loss } k_{11} = 120 \text{ s}^{-1} \text{ (fit)} \quad (11)$$

The wall losses of F atoms and SH radicals were measured directly, monitoring the loss of these species in the absence of other reactants in the reactor. When measuring k_{10}, the concentration of SH radicals (formed in Reaction (1) in an excess of H_2S) was relatively low (≈10^{11} molecule cm^{-3}) in order to minimize the contribution of the SH + SH reaction. Values of k_{10} measured at T = 220–960 K were in the range (20–35) s^{-1} with no notable correlation with temperature.

The data in Figure 5 show that the reaction mechanism used for the simulation gives an adequate representation of the chemical processes occurring in the reactor. The absolute concentrations of S atoms (detected as SBr, see Section 2) were not measured in the study; therefore, the corresponding experimental points in Figure 5 were simply scaled to the

simulated profile. In addition, a first-order S-atom loss rate of 120 s^{-1} was included in the mechanism to better match experimental data. In any case, the data on the S-atom are not involved in the determination of k_2 and are shown only for the sake of completeness.

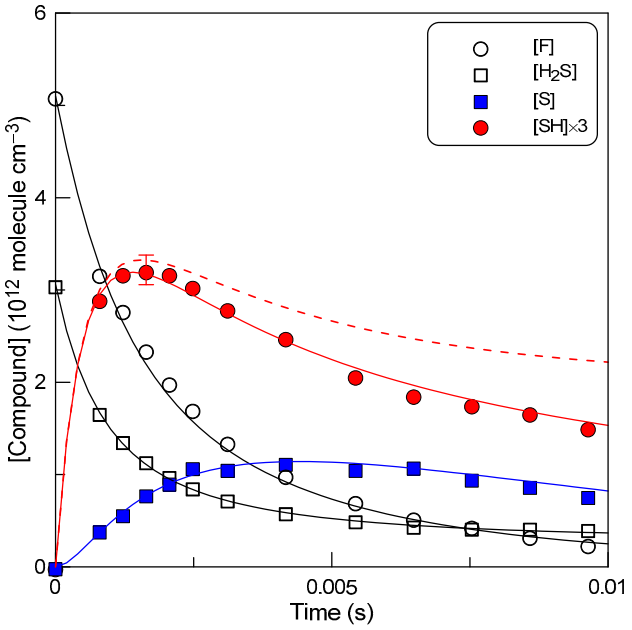

Figure 5. Reaction F + H_2S: measured (points) and simulated (lines) kinetics of the reactants (F and H_2S) and products (S and SH), T = 295 K.

One can note that the kinetics of two reactants, F-atom and H_2S, are well described with k_1, determined above in an excess of H_2S. The SH concentration, as expected, increases to a maximum and then drops due to the loss of SH in Reactions (2), (7) and (10). The dotted line in Figure 5 shows the SH profile calculated without taking into account the SH losses in its self-Reaction (7) and on the wall (10). The relative contribution of these reactions increases with the reaction time (as F-atom is consumed). At the maximum concentration of SH, the impact of these two reactions can be considered negligible (the error bar displayed at the top of the SH profile corresponds to 5%), even for the relatively high initial concentration of H_2S used in this experiment. Hence, one can conclude that the maximum concentration of SH is determined with a sufficient degree of accuracy by only two processes, the formation of SH in Reaction (1) and the consumption in Reaction (2), with $k_1[H_2S] = k_2[SH]_{max}$ at the time when [SH] is maximum. We did not perform the above analysis at other temperatures. It was assumed that the aforementioned conclusion is valid over the entire temperature range of the study, since the wall loss of SH does not vary significantly with temperature and the temperature dependence of the SH + SH reaction (unknown) is expected to be weak.

Thus, k_2 was determined relative to k_1 from the ratio $k_1/k_2 = [SH]_{max}/[H_2S]$. Experiments consisted of monitoring the concentrations of SH and H_2S when [SH] reached its maximum. Examples of the experimental data observed at three different temperatures with varied initial concentration of H_2S are shown in Figure 6. The slopes of the straight lines in Figure 6 provide the k_1/k_2 ratios at respective temperatures. The experimental conditions and the results of these measurements are summarized in Table 2. The values of k_2 presented in Table 2 were calculated using $k_1 = 1.86 \times 10^{-10}$ cm^3 $molecule^{-1}$ s^{-1} (T = 220–960 K), determined in the present work.

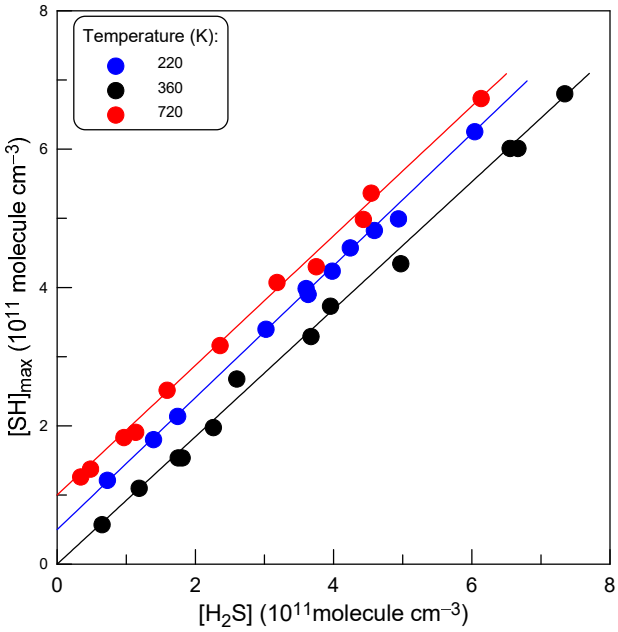

Figure 6. Typical dependence of $[SH]_{max}$ on $[H_2S]$ (see text). For clarity, the experimental points at T = 220 and 720 K are Y-shifted by 0.5 and 1, respectively.

Table 2. Experimental conditions and results of the measurements of the rate coefficient of Reaction (2).

T (K) [a]	$[H_2S]_0$ [b]	k_1/k_2 [c]	k_2 [d]	Reactor Surface [e]
220	0.22–1.81	0.95	1.96	HW
235	0.12–2.23	0.97	1.92	HW
250	0.19–2.07	1.01	1.84	HW
270	0.13–2.80	0.96	1.94	HW
295	0.18–3.42	0.97	1.92	HW
300	0.22–2.73	0.94	1.98	Q
320	0.57–4.59	0.84	2.21	HW
360	0.19–2.21	0.92	2.02	Q
410	0.17–2.17	0.86	2.16	Q
475	0.15–2.05	0.97	1.92	Q
575	0.12–2.14	0.85	2.19	Q
720	0.10–1.84	0.94	1.98	Q
960	0.07–1.28	0.91	2.04	Q

[a] 8–12 measurements with different $[H_2S]$ at each temperature; [b] Units of 10^{12} molecule cm^{-3}; [c] statistical 2σ uncertainty is $\leq$2.5%; [d] units of 10^{-10} cm^3 $molecule^{-1}$ s^{-1}, total estimated uncertainty is 25%; [e] HW: halocarbon wax; Q: quartz.

Temperature dependence of k_2 is shown in Figure 7. The only value of k_2 available in the literature is that reported by Schölne et al. [12]. The authors determined $k_2 = (2.0 \pm 0.4) \times 10^{-10}$ cm^3 $molecule^{-1}$ s^{-1} at T = 298 K from modeling SH kinetics in F + H_2S system under an excess of F atoms over H_2S. Fitting the current experimental data with an exponential function (solid line in Figure 7) yields the following Arrhenius expression: $k_2 = (2.14 \pm 0.09) \times 10^{-10} \exp(-(23 \pm 14)/T)$ cm^3 $molecule^{-1}$ s^{-1} with 2σ uncertainties representing the precision of the fit. The measured rate coefficient is observed to be independent of temperature, with all measured k_2-values well within their corresponding uncertainties, $k_2 = (2.0 \pm 0.4) \times 10^{-10}$ cm^3 $molecule^{-1}$ s^{-1}, in the temperature range of the measurements, T = 220–960 K. This value of k_2 is recommended from the present study with a conservative uncertainty of 20% (including the uncertainty on the rate coefficient of the reference reaction).

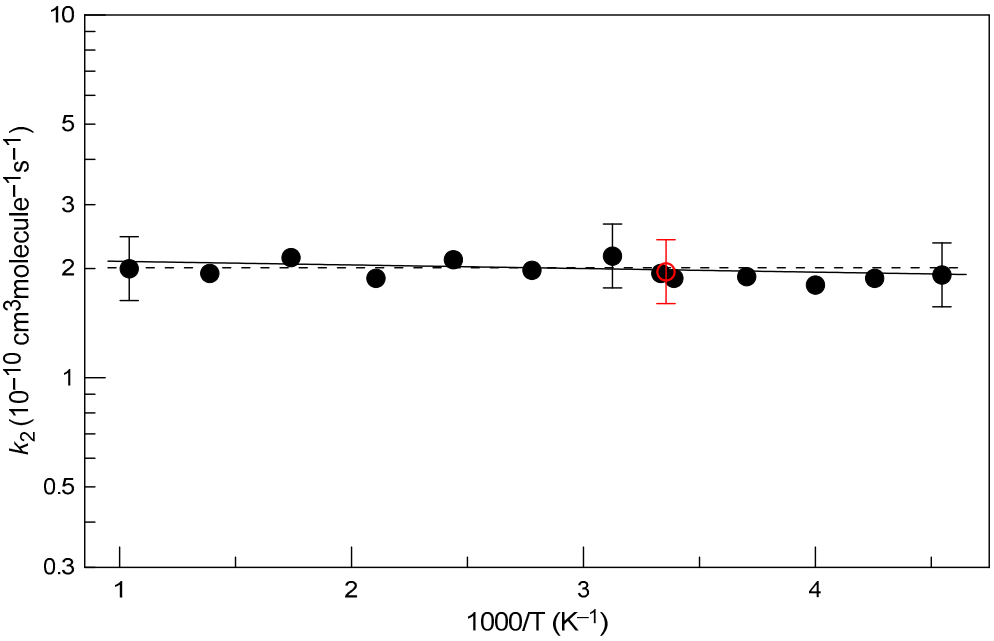

Figure 7. Temperature dependence of k_2: open red circle, Schölne et al. [12]; filled circle, this work. Uncertainties shown for selected present measurements of k_2 correspond to 20%.

4. Conclusions

In this work, using a discharge-flow reactor combined with mass spectrometry, we have investigated the kinetics of the reaction of atomic fluorine with hydrogen sulfide in a wide temperature range, 220–960 K. The F + H_2S reaction is an effective source of SH radical (important intermediate in atmospheric and combustion chemistry) in laboratory studies. The rate coefficient of this reaction measured for the first time as a function of temperature was found to be practically independent of temperature with the value of $k_1 = (1.86 \pm 0.28) \times 10^{-10}$ cm^3 molecule^{-1} s^{-1} at T = 220–960 K. Similar results were observed for the fast secondary reaction F + SH occurring in the F + H_2S chemical system: $k_2 = (2.0 \pm 0.4) \times 10^{-10}$ cm^3 molecule^{-1} s^{-1} at the same temperature range. The rate coefficient data for F atom reactions with H_2S and SH obtained for the first time in an extended temperature range provide an experimental dataset for use in laboratory studies and theoretical reaction rate calculations.

Funding: This research was funded by ANR through the PIA (Programme d'Investissement d'Avenir). Grant number ANR-10-LABX-100-01.

Institutional Review Board Statement: Not applicable.

Informed Consent Statement: Not applicable.

Data Availability Statement: The data supporting reported results are available in this article.

Acknowledgments: Support from the VOLTAIRE project (ANR-10-LABX-100-01) funded by ANR is gratefully acknowledged.

Conflicts of Interest: The author declares no conflict of interest.

References

1. Manion, J.A.; Huie, R.E.; Levin, R.D.; Burgess, D.R.; Orkin, V.L.; Tsang, W.; McGivern, W.S.; Hudgens, J.W.; Knyazev, V.D.; Atkinson, D.B.; et al. *NIST Chemical Kinetics Database, NIST Standard Reference Database 17*; Version 7.0 (Web Version), Release 1.6.8, Data Version 2015.12; National Institute of Standards and Technology: Gaithersburg, Maryland, 2022. Available online: http://kinetics.nist.gov/ (accessed on 20 October 2022).
2. Stevens, P.S.; Brune, W.H.; Anderson, J.G. Kinetic and Mechanistic Investigations of F + H_2O/D_2O and F + H_2/D_2 over the Temperature Range 240–373 K. *J. Phys. Chem.* **1989**, *93*, 4068–4079. [CrossRef]

3. Walther, C.-D.; Wagner, H.G. Über Die Reaktionen Von F-Atomen Mit H_2O, H_2O_2 Und NH_3. *Ber. Bunsenges. Phys. Chem.* **1983**, *87*, 403–409. [CrossRef]
4. Bedjanian, Y. Rate Constant of the Reaction of F Atoms with Methane over the Temperature Range 220–960 K. *Chem. Phys. Lett.* **2021**, *770*, 138458. [CrossRef]
5. Bedjanian, Y. Temperature-Dependent Rate Constant for the Reaction of F Atoms with HNO_3. *Int. J. Chem. Kinet.* **2019**, *51*, 753–759. [CrossRef]
6. Hynes, A.J.; Wine, P.H. Kinetics and Mechanisms of the Oxidation of Gaseous Sulfur Compounds. In *Gas-Phase Combustion Chemistry*; Gardiner, W.C., Ed.; Springer New York: New York, NY, USA, 2000; pp. 343–388.
7. Tyndall, G.S.; Ravishankara, A.R. Atmospheric Oxidation of Reduced Sulfur Species. *Int. J. Chem. Kinet.* **1991**, *23*, 483–527. [CrossRef]
8. Kornweitz, H.; Persky, A. Modeling the F + H_2S Reaction with an F + HS Potential. *Chem. Phys. Lett.* **1999**, *307*, 479–483. [CrossRef]
9. Williams, R.L.; Rowland, F.S. Hydrogen Atom Abstraction by Fluorine Atoms. *J. Phys. Chem.* **1973**, *77*, 301–307. [CrossRef]
10. Smith, D.J.; Setser, D.W.; Kim, K.C.; Bogan, D.J. HF Infrared Chemiluminescence. Relative Rate Constants for Hydrogen Abstraction from Hydrocarbons, Substituted Methanes, and Inorganic Hydrides. *J. Phys. Chem.* **1977**, *81*, 898–905. [CrossRef]
11. Persky, A. Kinetics of the Reactions F + H_2S and F + D_2S at 298 K. *Chem. Phys. Lett.* **1998**, *298*, 390–394. [CrossRef]
12. Schönle, G.; Rahman, M.M.; Schindler, R.N. Kinetics of the Reaction of Atomic Fluorine with H_2S and Elementary Reactions of the HS Radical. *Ber. Bunsenges. Phys. Chem.* **1987**, *91*, 66–75. [CrossRef]
13. Bedjanian, Y.; Lelièvre, S.; Le Bras, G. Kinetic and Mechanistic Study of the F Atom Reaction with Nitrous Acid. *J. Photochem. Photobio. A* **2004**, *168*, 103–108. [CrossRef]
14. Bedjanian, Y. Kinetics and Products of the Reactions of Fluorine Atoms with ClNO and Br_2 from 295 to 950 K. *J. Phys. Chem. A* **2017**, *121*, 8341–8347. [CrossRef] [PubMed]
15. Bedjanian, Y. Reaction F + C_2H_4: Rate Constant and Yields of the Reaction Products as a Function of Temperature over 298–950 K. *J. Phys. Chem. A* **2018**, *122*, 3156–3162. [CrossRef] [PubMed]
16. Bedjanian, Y. Rate Constants for the Reactions of F Atoms with H_2 and D_2 over the Temperature Range 220-960 k. *Int. J. Chem. Kinet.* **2021**, *53*, 527–535. [CrossRef]
17. Morin, J.; Romanias, M.N.; Bedjanian, Y. Experimental Study of the Reactions of OH Radicals with Propane, *n*-Pentane, and *n*-Heptane over a Wide Temperature Range. *Int. J. Chem. Kinet.* **2015**, *47*, 629–637. [CrossRef]
18. Nesbitt, F.L.; Cody, R.J.; Dalton, D.A.; Riffault, V.; Bedjanian, Y.; Le Bras, G. Temperature Dependence of the Rate Constant for the Reaction $F(^2P)$ + Cl_2 → FCl + Cl at T = 180–360 K. *J. Phys. Chem. A* **2004**, *108*, 1726–1730. [CrossRef]
19. Clyne, M.A.A.; Townsend, L.W. Rate Constant Measurements for Rapid Reactions of Ground State Sulphur 3p4(3pj) Atoms. *Int, J. Chem. Kinet.* **1975**, *39*, 73.
20. Burkholder, J.B.; Sander, S.P.; Abbatt, J.; Barker, J.R.; Cappa, C.; Crounse, J.D.; Dibble, T.S.; Huie, R.E.; Kolb, C.E.; Kurylo, M.J.; et al. Chemical Kinetics and Photochemical Data for Use in Atmospheric Studies, Evaluation No. 19, JPL Publication 19-5, Jet Propulsion Laboratory. Available online: http://jpldataeval.jpl.nasa.gov (accessed on 20 October 2022).
21. Mihelcic, D.; Schindler, R.N. ESR-Spektroskopische Untersuchung Der Reaktion Von Atomarem Wasserstoff Mit H_2S. *Ber. Bunsenges. Phys. Chem.* **1970**, *74*, 1280–1288.
22. Bradley, J.N.; Trueman, S.P.; Whytock, D.A.; Zaleski, T.A. Electron Spin Resonance Study of the Reaction of Hydrogen Atoms with Hydrogen Sulphide. *J. Chem. Soc. Faraday Trans. 1* **1973**, *69*, 416–425. [CrossRef]